Lawrence Berkeley National Laboratory
Recent Work

Title
ATOMIC CROSS SECTION EFFECTS IN SOFT X-RAY PHOTOEMISSION FROM Ag VALENCE BANDS

Permalink
https://escholarship.org/uc/item/06g3c0p4

Author
Wehner, P.S.

Publication Date
1976-04-01

eScholarship.org Powered by the California Digital Library
University of California

0 0 0 0 4 3 0 4 0 5 8

Submitted to Physical Review B

LBL-4985
Preprint

ATOMIC CROSS SECTION EFFECTS IN SOFT X-RAY PHOTOEMISSION FROM Ag VALENCE BANDS

P. S. Wehner, J. Stöhr, G. Apai, F. R. McFeely,
R. S. Williams, and D. A. Shirley

April 1976

Prepared for the U. S. Energy Research and
Development Administration under Contract W-7405-ENG-48

For Reference

Not to be taken from this room

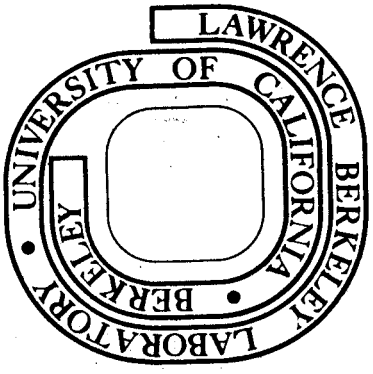

LBL-4985
c.1

DISCLAIMER

This document was prepared as an account of work sponsored by the United States Government. While this document is believed to contain correct information, neither the United States Government nor any agency thereof, nor the Regents of the University of California, nor any of their employees, makes any warranty, express or implied, or assumes any legal responsibility for the accuracy, completeness, or usefulness of any information, apparatus, product, or process disclosed, or represents that its use would not infringe privately owned rights. Reference herein to any specific commercial product, process, or service by its trade name, trademark, manufacturer, or otherwise, does not necessarily constitute or imply its endorsement, recommendation, or favoring by the United States Government or any agency thereof, or the Regents of the University of California. The views and opinions of authors expressed herein do not necessarily state or reflect those of the United States Government or any agency thereof or the Regents of the University of California.

0 0 0 0 4 5 0 4 0 6 9

ATOMIC CROSS SECTION EFFECTS IN SOFT X-RAY PHOTOEMISSION FROM Ag VALENCE BANDS*

P. S. Wehner, J. Stöhr, G. Apai, F. R. McFeely,
R. S. Williams, and D. A. Shirley

Materials and Molecular Research Division
Lawrence Berkeley Laboratory

and

Department of Chemistry
University of California
Berkeley, California 94720

April 1976

ABSTRACT

The relative photoemission intensity from the Ag 4d valence band (VB) was studied as a function of photon energy using 32 - 250 eV synchrotron radiation. A sharp decrease in intensity of more than an order of magnitude was observed in the range 100 eV $< \hbar\omega <$ 140 eV. At $\hbar\omega$ = 140 eV the 4d cross-section exhibits a minimum which is attributed to the radial node in the 4d wavefunction. High resolution VB spectra were obtained in the energy range 60 eV $\leqslant \hbar\omega \leqslant$ 150 eV. For 110 eV $\leqslant \hbar\omega \leqslant$ 130 eV the relative heights of the two prominent valence band peaks are inverted. This modulation is attributed to the strong variation of the atomic Ag 4d photoelectric cross section in this energy range. These results demonstrate the importance of carrying photoemission studies of 4d group metals to the $\hbar\omega \geqslant$ 150 eV range in order to bridge the UPS-to-XPS gap.

0 0 0 0 4 5 0 4 0 7 0

I. INTRODUCTION

The potential of synchrotron radiation for photoemission studies of solids has long been recognized. So far, however, most studies have been restricted to the photon energy range $\hbar\omega < 100$ eV.[1] The Stanford Synchrotron Radiation Project (SSRP),[2] on the storage ring SPEAR at the Stanford Linear Accelerator (SLAC), is uniquely capable of producing variable-energy photon beams of energies up to 250 eV in sufficient intensity and resolution for photoemission spectroscopy. Here we report a study of the valence band of Ag(4d) in the photon energy range 32 - 250 eV.

The present report may be regarded as a continuation of an earlier paper on polycrystalline Cu,[3] (hereafter referred to as I). The main emphasis of I was the study of cross-section effects which arise from the details of the initial- and final-state band structure and the transition matrix element. While such "band-structure-type" cross-section effects are also anticipated for Ag, an additional "atomic-type" cross section effect may be expected. The latter arises from the radial node in the Ag 4d wavefunction. It is known from atomic calculations[4] that so-called "Cooper minima"[5,6] exist in the cross section for initial state wavefunctions which exhibit a radial node. In such cases the cross section may vary strongly over a small energy range. One objective of the present paper is to investigate whether such effects can be observed in photoemission from the Ag valence band. Two different kinds of measurements are reported. First we investigate the variation of the effective total photoelectron intensity from the 4d valence band in the photon energy range 32 eV $\leq \hbar\omega \leq$ 250 eV.

Secondly, we report high resolution VB spectra in the energy range 60 eV $\leq \hbar\omega \leq$ 150 eV. The two sets of results are then combined and interpretated to deduce how the detailed shape of the VB is affected by atomic-type cross section effects.

II. EXPERIMENTS

Experiments were performed using synchrotron radiation from the storage ring SPEAR at SLAC.[2] The incident monochromatic[7] light was focused onto the silver samples which were positioned in the focal point of a double-pass cylindrical mirror analyzer (CMA). The polycrystalline Ag samples were prepared by *in situ* evaporation from a tungsten filament onto a stainless-steel substrate. The base pressure in the sample chamber was $\sim$1 x 10^{-9} Torr, with a maximum pressure of 2 x 10^{-8} during evaporation. The energy distributions of the photoemitted electrons were analyzed by operating the CMA in the retarding mode.[8] The kinetic energy of the photoelectrons is modified by a retarding (accelerating) voltage such that only those electrons are detected which have the correct pass energy (E_p) of the analyzer. For a given E_p the resolution ΔE of the CMA is fixed. The variation of the total Ag 4d intensity with photon energy was studied with an analyzer resolution of ΔE = 1.6 eV, at E_p = 100 eV. High resolution VB spectra were recorded with a resolution of ΔE = 0.35 eV, at E_p = 50 eV.[9]

III. RESULTS

Results of our high resolution studies of the Ag valence bands in the photon energy range 60 eV $\leq h\nu \leq$ 150 eV are shown in Fig. 1.

0 0 0 0 4 5 0 4 0 7 1

Characteristic features are the flat s-band extending beyond 3 eV binding energy (BE) below the Fermi level and the two prominent d-peaks centered at ∿4.8 eV and ∿6.3 eV BE, respectively. At the lowest and highest photon energies the d-band structure resembles roughly the x-ray photoemission spectrum (XPS) in Fig. 2 which was taken with Aℓ Kα (1486.6 eV) radiation on a Hewlett-Packard 5950A spectrometer. The s-band intensity of all spectra in Fig. 1 is reduced relative to the XPS result, by a factor of approximately 3. The most prominent changes in the shape of the 4d valence band occur in the energy range 110 eV - 130 eV. Here, the relative heights of the two leading d-peaks are inverted relative to the lower and higher photon energy range.[10]

The variation of the Ag 4d intensity with photon energy shown in Fig. 3, was derived in the following way. The experimental spectra were corrected for their inelastic background. The Ag 4d peak region was defined as 3 eV $\leq$ BE $\leq$ 8 eV. The intensity of the s-band in this energy range was estimated by extrapolating the s-band intensity for EB $<$ 3 eV and subtracted from the total intensity. The area obtained this way for the 4d band was normalized with respect to the average photon flux incident on the sample. The photon flux depends on both the electron-beam current of SPEAR at the time of measurement and the transmission of the mirror plus monochromator assembly at a given photon energy. The beam current and its decay during data collection (typical time ∿30 minutes per spectrum) was supplied on line by SPEAR. The transmission of the mirror plus monochromator as a function of photon energy had previously been measured with a sodium salicylate scintillation counter.[11] Finally,

the data were corrected for the collecting efficiency of the CMA.[8,12,13] Due to the action of the accelerating/retarding field the collecting efficiency is a function of both the pass energy (E_p) and the kinetic energy (E_k) of the electrons emitted from the sample. The transmitted current in general is theoretically given by $I \sim E_p/E_k$.[8,12] Thus the observed 4d intensity at a given photon energy $\hbar\omega$ was corrected by a factor E_k/E_p where in our case E_p = 100 eV and $E_k = \hbar\omega$ - 10 eV (4d binding energy + work function = 10 eV). As seen from Fig. 3 the experimental error bars of our data points are rather small ($\sim\pm$10%). The largest uncertainty is the correction for the CMA collecting efficiency. The effect of this correction is seen from Fig. 3 where the uncorrected (constant collecting efficiency) 4d intensity is shown for comparison as a dashed line.

IV. DISCUSSION

Let us first discuss the variation of the Ag 4d intensity with photon energy. The measured intensity of the Ag valence band at a given photon energy ($I(\omega)$) is in general a very complex quantity. Among other factors that modulate $I(\omega)$ is the effect of electron energy loss during transport to the surface. This effect is most important in just the energy range we have studied. However, it is difficult to assess and is probably a much weaker effect than the atomic cross-section modulation discussed below (the escape depth probably varies by a factor of 2 or less, while the atomic cross-section varies over an order of magnitude). We shall therefore consider the variation in mean escape depth to be absorbed in an "effective" cross-section variation. For the case of an angle integrated measurement on a

0 0 0 0 4 5 0 4 0 7 2

polycrystalline sample the observed intensity in this approximation is given by[14]

$$I(\omega) = \frac{C}{\omega}\int dE\ N(\omega,E)$$
$$= \frac{C}{\omega}\int dE \int d^3k \sum_{f,j} |t_{fj}(\vec{k})|^2\ \delta(E_f(\vec{k}) - E_j(\vec{k}) - \hbar\omega)\ \delta(E - E_j(\vec{k})) \qquad (1)$$

Here $N(\omega,E)$ is the photoemission energy distribution (PED) that is usually measured in photoemission experiments (cp. Fig. 1). $t_{fj}(\vec{k})$ is a momentum matrix element for a transition between an initial state j of energy $E_j(\vec{k})$ and a final state f of energy $E_f(\vec{k})$. The $\vec{k}$-integration extends over the first Brillouin zone (BZ). From equation (1) it is seen that it is in general impossible to relate the measured quantity $I(\omega)$ to a single physical parameter. However, such a correspondence can be approximately established if <u>final</u> state effects are weak, i.e. if transitions are allowed throughout the whole BZ and effects arising from the <u>angular</u> part[3] of the matrix element t_{fj} are unimportant. In this case equation (1) simplifies to[15]

$$I(\omega) = \frac{C}{\omega}\int dE\ \overline{|t_{fj}|^2}\ N_j(E)\ N_f(E + \hbar\omega) \qquad (2)$$

Here $\overline{|t_{fj}|^2}$ is an angle averaged (radial) transition matrix element which depends on the wavevector of the photoelectron $|\vec{q}| = \sqrt{2m\ (E + \hbar\omega)}\ /\hbar$.[16] $N_j(E)$ and $N_f(E + \hbar\omega)$ are the initial and final densities of states, respectively. To a good approximation it can usually be assumed that $|t_{fj}|^2$ and N_f are only weakly energy dependent over the range of integration, i.e. over the width of the valence

band ($\sim$3 eV), provided that the photon energy is sufficiently high. Then the measured intensity is directly proportional to the photoionization cross section

$$I(\omega) \sim \sigma(\omega, E_f) \sim \frac{1}{\omega} \overline{|t_{fj}(E_f)|^2}\, N_f(E_f) \quad . \tag{3}$$

Here $E_f = \bar{E}_j + \hbar\omega$, and $\bar{E}_j$ is taken to be the center of the 4d valence band. $\sigma(\omega)$ has been calculated for various atoms.[4] Unfortunately, at present, no experimental or reliable theoretical results are available for atomic Ag 4d orbitals. A comparison of accurate theoretical atomic cross-sections with the present data might yield useful information on how cross-section effects are modified when the atom is introduced into a solid. In fact, from our previous results for polycrystalline Cu[3] one would expect final state band structure effects to be weak for $h\nu \geqslant 80$ eV, and therefore equation (3) should hold to a reasonable approximation. In the range $h\nu \leqslant 80$ eV the curve in Fig. 4 might deviate from a corresponding plot of the atomic Ag 4d cross section versus energy because the final state band structure and effects due to the angular part of the transition matrix element come into play.[3] However, since such deviations are closely related to the weak modulation effects seen in extended x-ray absorption fine structure (EXAFS), they might lie within the error bars of our measurement.

The minimum in the curve shown in Fig. 4 arises from the radial matrix element $\overline{|t_{fj}|^2}$ in equation (3)[17] and may be explained as follows. The selection rules for electric dipole transitions $\Delta\ell = \pm 1$ connect the 4d initial state of Ag to p- and f-partial wave final states. In general, a minimum in the cross section can occur provided

0 0 0 0 4 5 0 4 0 7 3

the initial state wavefunction has at least one node. In this case the radial dipole matrix element associated with the p or the f channel may change sign as a function of photon energy.[18] The photoexcitation cross section, which is proportional to the sum of the square of the matrix elements, will then exhibit a minimum at the energy for which one of the matrix elements vanishes. Because the absolute value of the d → f matrix element dominates the d → p one at higher (> 20 eV) energies[6] the minimum observed for Ag 4d at $\hbar\omega$ = 140 eV may be attributed to a vanishing d → f matrix element at this energy. We have calculated the Ag 4d cross-section as a function of the kinetic energy of the photoelectron, using plane-wave (PW) and orthogonalized plane-wave (OPW) final states for the continuum electron.[19] The results of such calculations for $\overline{|t_{fj}|^2}$ are shown in Fig. 4 for the cases of Cu(3d) and Ag(4d). While neither PW nor OPW can be taken seriously for quantitative estimates of cross-sections, we note that both show deep minima around $\hbar\omega$ = 140 eV for Ag. For Cu no such minimum exists. In the simple PW and OPW final state picture the correspondence between a minimum in the cross section and a radial node in the initial state wavefunction is easily seen. Consider the atomic matrix element for a 3d and a 4d initial state wavefunction and a PW final state:

$$< e^{i\vec{q}\cdot\vec{r}} \; |\vec{p}| \; ar^2e^{-\alpha r} + br^3e^{-\beta r} > \qquad (4)$$

Here $\vec{q}$ is the photoelectron wavevector, and the initial state is written in form of Slater orbitals. For a 3d initial state: $a > 0$, $b \geq 0$. For 4d: $a > 0$, $b < 0$, and a radial node exists. Thus, for a 3d state

both parts of the matrix element in equation (4) have the same sign. For a 4d state opposite signs result, and, depending on the magnitude of the two terms the matrix element (4) may change sign as a function of the final state energy ($\sim|\vec{q}|^2$). The square of the matrix element then exhibits a Cooper minimum. While for a PW final state the cross-section in a Cooper minimum is zero, it is finite for an OPW due to the orthogonalization terms in the matrix element.[3]

In the context of the present paper the curve shown in Fig. 3 is of interest for yet another reason, namely, for its effect on the detailed shape of the VB spectrum (Fig. 1). In particular, we focus our attention on the changes in the energy range 90 eV $\leq \hbar\omega \leq$ 150 eV. At these photon energies "band-structure-type" cross section effects are expected to be weak[3] and may therefore be excluded as being responsible for the observed inversion of peak intensites for 110 $\leq \hbar\omega \leq$ 130 eV. On the other hand, the curve shown in Fig. 3 exhibits its largest slope exactly in this latter energy range. As is seen from equation (3) this curve describes in good approximation the dependence of the 4d cross section on the final state kinetic energy $E_f = \hbar\omega + E_j$.[20] Earlier, in discussing the <u>energy integrated</u> quantity $I(\omega)$ we neglected the dependence of t_{fj} and N_f on E_j (equation (3)) by introducing an averaged value $\overline{E}_j$. For the <u>energy resolved</u> PED's taken at a fixed $\hbar\omega$ the curve in Fig. 3 describes the variation of $\sigma(\omega, E_f)$ over the range of the valence band energies E_j. In the range of steepest slope, i.e. for 100 eV $\leq \hbar\omega \leq$ 130 eV, changes of approximately 20% in $\sigma(\omega, E_f)$ result over an energy interval of

0 0 0 0 4 5 0 4 0 7 4

$\Delta E_j \sim 2$ eV, which is approximately the separation of the two prominent VB peaks (Fig. 1).[21] Thus in this energy range the effect of the radial matrix element[17] on the detailed shape of the valence band is not negligible. Neglecting "band-structure-type" cross section effects the PED at a given photon energy is described by

$$N(\omega, E) = C \int d^3k \sum_j \sigma(\omega, E_f) \quad \delta(E - E_j(\vec{k})) \quad . \qquad (5)$$

Fig. 5 shows the results of a calculation using equation (5). The solid curve corresponds to the case $\sigma(\omega, E_f)$ = const; i.e. to the density of (initial) states. Details of the calculation are described in I. Smith's[22] parameters were used with a spin orbit coupling of 0.015 Ry included. The dashed curve was calculated by including the dependence of $\sigma(\omega, E_f)$ on the final state energy. The calculation corresponds to $\hbar\omega$ = 120 eV. The dependence of $\sigma(\omega, E_f)$ was taken from Fig. 3. Including a final state energy dependent cross section enhances the high BE peak of the Ag 4d valence band by a maximum of 17%. We believe that this effect is responsible for the observed changes in the shape of the valence-band spectrum in the range 90 - 150 eV. When comparing the slope of the curve in Fig. 3 with the intensity ratio of the two prominent valence band peaks in Fig. 1, the close relationship is apparent.

We conclude that in the case of polycrystalline silver, even with all the averaging effects that are implied by polycrystallinity and angle-integrated electron detection in our CMA, the transition from a UPS-like to an XPS-like 4d-band spectrum is not complete

before 150 eV. If our spectra had been taken with photon energies extending only up to 90 eV, the reversal of intensities would have been overlooked; if to 110 eV, an incorrect density of states might have been inferred. Similar behavior may be expected in other 4d-group elements. It therefore seems important that valence-band studies on these elements be carried out with photon energies up to at least 150 eV.

We note in passing that Lindau et. al. have observed an inversion of the two peaks in the 5d valence band of gold.[23] We have not considered this result here because we believe its origins are somewhat more complicated. It will be discussed in a forthcoming paper on angle-resolved photoemission from gold.[24]

Finally, we briefly comment on band structure type cross section effects which are expected for $\hbar\omega \leq 80$ eV. A close inspection of the spectra in Fig. 1 reveals that the high BE peak is reduced for $\hbar\omega \leq 80$ eV relative to the XPS result (shown in Fig. 2) which should closely represent the initial density of states.[3] This becomes even more apparent when the influence of the inelastic background is taken into account. Similar effects have also been observed in I for Cu in the 50 - 70 eV range, although the spectral changes are more dramatic for Cu. Also, for Cu the strongest decrease in intensity of the high BE side was observed for $50 \text{ eV} \leq \hbar\omega \leq 60$ eV while for Ag the high BE side is lowest for $\hbar\omega = 80$ eV. The fact that band structure type cross section effects for Ag are weak at the lowest energies studied seems to confirm our interpretation of the effects observed at higher photon energies.

0 0 0 0 4 5 0 4 0 7 5

ACKNOWLEDGEMENTS

We would like to thank R. Z. Bachrach and the Xerox group, Palo Alto, for the use of their experimental apparatus and for experimental help during the initial phase of the project.

One of us (J. S.) would like to acknowledge the Deutsche Forschungs-gemein-Schaft for granting a stipend.

FOOTNOTES AND REFERENCES

*This work was performed at the Stanford Synchrotron Radiation Project, which is supported by the National Science Foundation Grant No. DMR 73-07692 A02, in cooperation with the Stanford Linear Accelerator Center. Our research is supported by the U. S. Energy Research and Development Administration. The electron analyzer was purchased by funds obtained from NSF Grant No. GH-40132.

1. For a review see D. E. Eastman in Vacuum Ultraviolet Radiation Physics, Edit. E. E. Koch, R. Haensel, and C. Kunz (Pergamon, Vieweg 1974) p. 417.
2. H. Winick, in reference 1, p. 776.
3. J. Stöhr, F. R. McFeely, G. Apai, P. S. Wehner, and D. A. Shirley, submitted to Phys. Rev. B.
4. D. J. Kennedy and S. T. Manson, Phys. Rev. A5, 227 (1972).
5. J. W. Cooper, Phys. Rev. Lett. 13, 762 (1964).
6. U. Fano and J. W. Cooper, Rev. Mod. Phys. 40, 441 (1968).
7. F. C. Brown, R. Z. Bachrach, S. B. M. Hagström, N. Lien, and C. H. Pruett in reference 1, p. 785.
8. P. W. Palmberg, J. Electron Spectrosc. 5, 691 (1974).
9. Low (ΔE = 1.6 eV) and high (ΔE = 0.35 eV) resolution spectra were taken with two different CMA's with $\Delta E/E_p$ = 1.6% and 0.7% respectively.
10. The rather poor statistics of the spectrum at $\hbar\omega$ = 150 eV is due to a low cross section of the VB in this region (cp. Figure 3).
11. We are grateful to I. Lindau and P. Pianetta for supplying their results on the monochromator transmission function.

0 0 0 0 4 5 0 4 0 7 6

12. J. C. Helmer and N. H. Weichert, Appl. Phys. Lett. 13, 266 (1968).

13. J. L. Gardner and J. A. R. Samson, J. Electron Spectrosc. 2, 267 (1973).

14. See for example reference 1. At the photon energies of this study transport and escape terms may be neglected (cp. reference 3). We have explicity included a factor $1/\omega$ in equation (1) which normalizes $N(\omega, E)$ with respect to the incident photon flux.

15. This is easily derived if the selection rules of $\vec{k}$-conservation are ignored and a continuum of final states is assumed. Although it is known that $\vec{k}$-conservation is in general an important selection rule, equation (2) is still approximately correct at photon energies where final state momentum broadening is important or for the case that the number of final Bloch states is sufficient to lead to an effective angular integration of the transition matrix element (cp. reference 3). Note, however, that the above statements apply only to angle integrated photoemission from polycrystalline samples.

16. See equation (A17) in reference 3. Here we have neglected the wavevector dependence of $\overline{|t_{fj}|^2}$, i.e. we have assumed $\sum_m |a_m^j(\vec{k})|^2 = \text{const.}$

17. The final density of states $N_f(E_f) = (E_f)^{1/2}$ cannot be responsible for the strong variations of the curve in Fig. 3.

18. See for example A. M. Msezane and S. T. Manson, Phys. Rev. Lett. 35, 364 (1975) and references 5 and 6.

19. We have used equation (A17) in reference 3 with $\sum_{m} |a_m^j(\vec{k})|^2 = 1$. The coefficients for the 3d and 4d wavefunctions in form of single zeta Slater orbitals were taken from: E. Clementi and C. Roetti, Atomic Data and Nuclear Data Tables 14, 177 (1974).

20. E_f differs from the kinetic energy of the photoelectron outside the crystal by a work function ($\sim$4.5 eV for Ag). The energies E_j and E_f are measured relative to the Fermi level $E_F = 0$.

21. Note that the slope of the curve in Fig. 3 in the range 100 eV $\leq \hbar\omega \leq$ 130 eV is almost unaffected by the correction for the analyzer transmission which is somewhat uncertain.

22. N. V. Smith, Phys. Rev. B3, 1862 (1971).

23. I. Lindau, P. Pianetta, K. Y. Yu, and W. E. Spicer, Phys. Rev. B13, 492 (1976).

24. J. Stöhr, G. Apai, P. S. Wehner, F. R. McFeely, R. S. Williams, and D. A. Shirley, to be published.

0 0 0 0 4 5 0 4 0 7 7

FIGURE CAPTIONS

Fig. 1. Photoemission spectra of Ag (polycrystalline) valence bands in the photon energy range 60 eV $\leq \hbar\omega \leq$ 150 eV. Experimental resolution was 0.35 eV.

Fig. 2. Photoemission spectrum of Ag valence bands at $\hbar\omega$ = 1486.6 eV (Aℓ Kα). Experimental resolution was ∿0.6 eV.

Fig. 3. Relative intensity of the Ag 4d peak as a function of photon energy. The data were collected during three different beam periods (Run 1, 2, 3). The dashed curve does not include the correction for the collecting efficienty of the cylindrical mirror analyzer as discussed in the text.

Fig. 4. Square of the radial matrix element $\overline{|t_{fj}|^2}$ (reference 19) as a function of the final state kinetic energy E_f (reference 20) for Cu (3d) and Ag (4d). PW and OPW mean plane-wave and orthogonalized plane-wave final states, respectively. The units of $\overline{|t_{fj}|^2}$ are arbitrary but the relative values for Cu and Ag are acurate. The energy scales of Fig. 3 ($\hbar\omega$) and Fig. 4 (E_f) differ by the average initial state energy $\overline{E}_j$ = - 5.5 eV.

Fig. 5. Calculation of the Ag 4d PED according to equation (5). The solid line is the density of (initial) states. The dashed curve takes the cross-section dependence on the final state energy $E_f = \hbar\omega + E_j$ into account (Fig. (3)) and corresponds to $\hbar\omega$ = 120 eV.

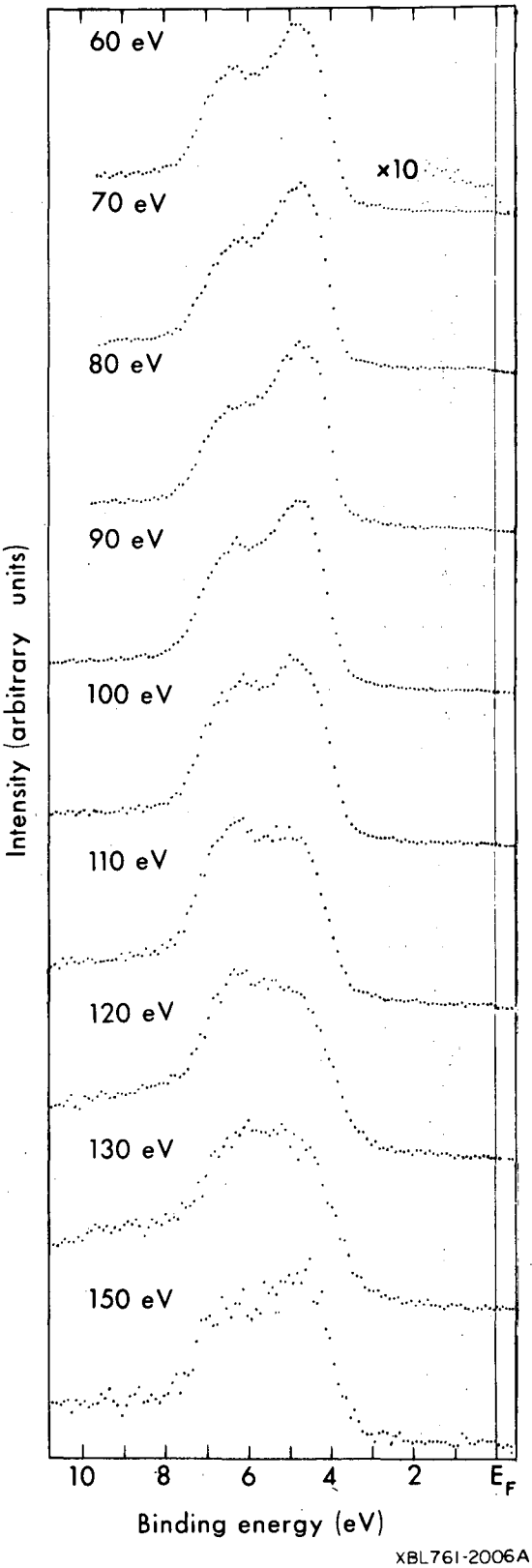
60 eV
×10
70 eV
80 eV
90 eV
100 eV
110 eV
120 eV
130 eV
150 eV
Intensity (arbitrary units)
10
8
6
4
2
E_F
Binding energy (eV)
XBL761-2006A

Fig. 1

0 0 0 0 4 5 0 4 0 7 8

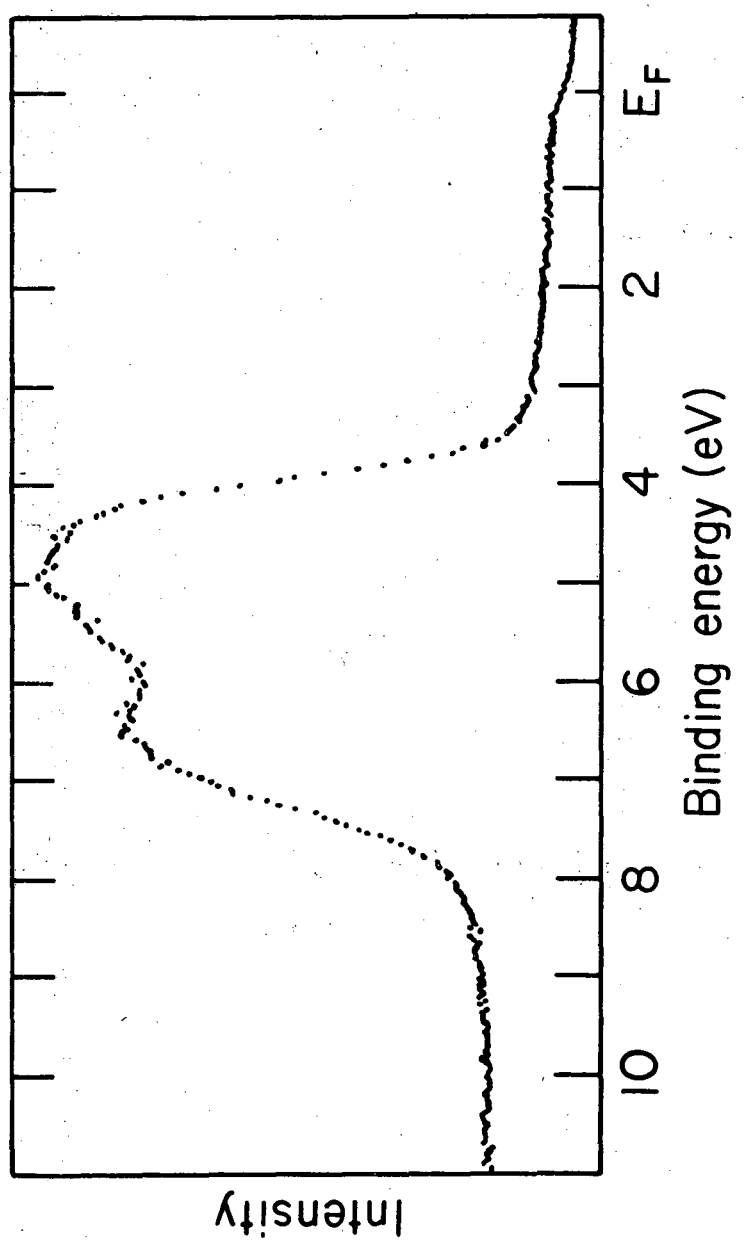

Fig. 2

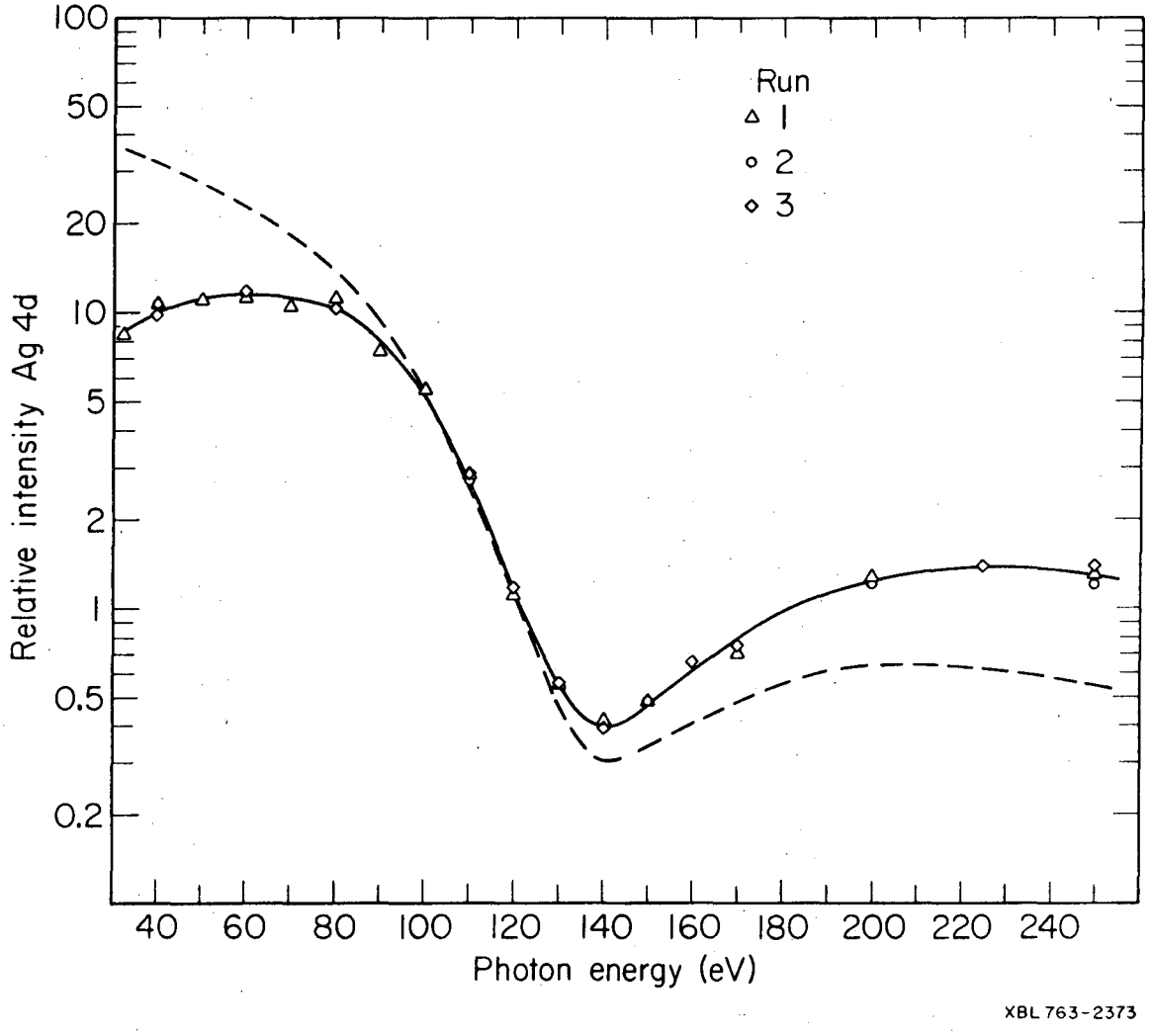
Relative intensity Ag 4d
100
50
20
10
5
2
1
0.5
0.2
Run
1
2
3
40
60
80
100
120
140
160
180
200
220
240
Photon energy (eV)
XBL 763-2373

Fig. 3

0 0 0 0 4 5 0 4 0 7 9

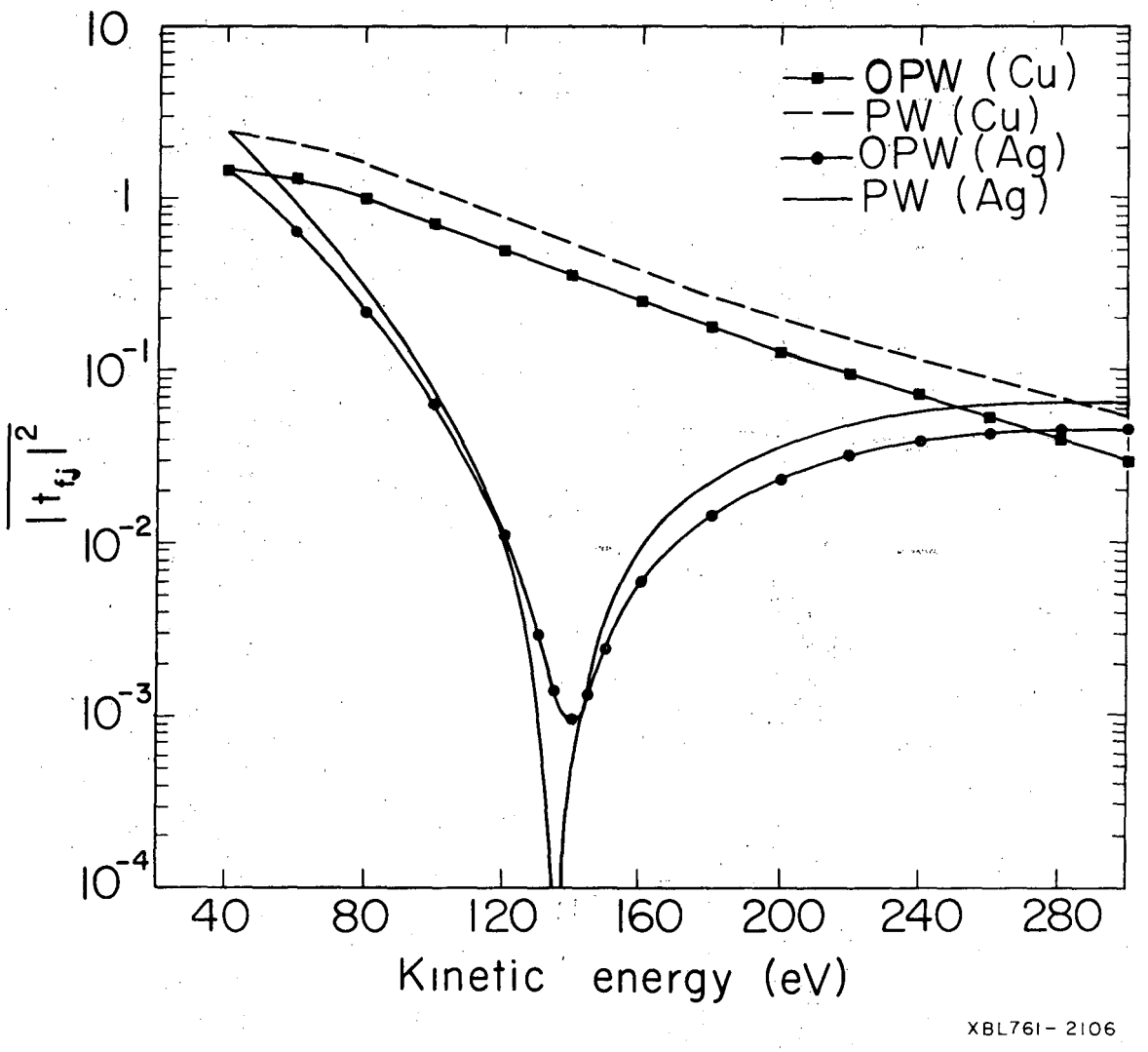

Fig. 4

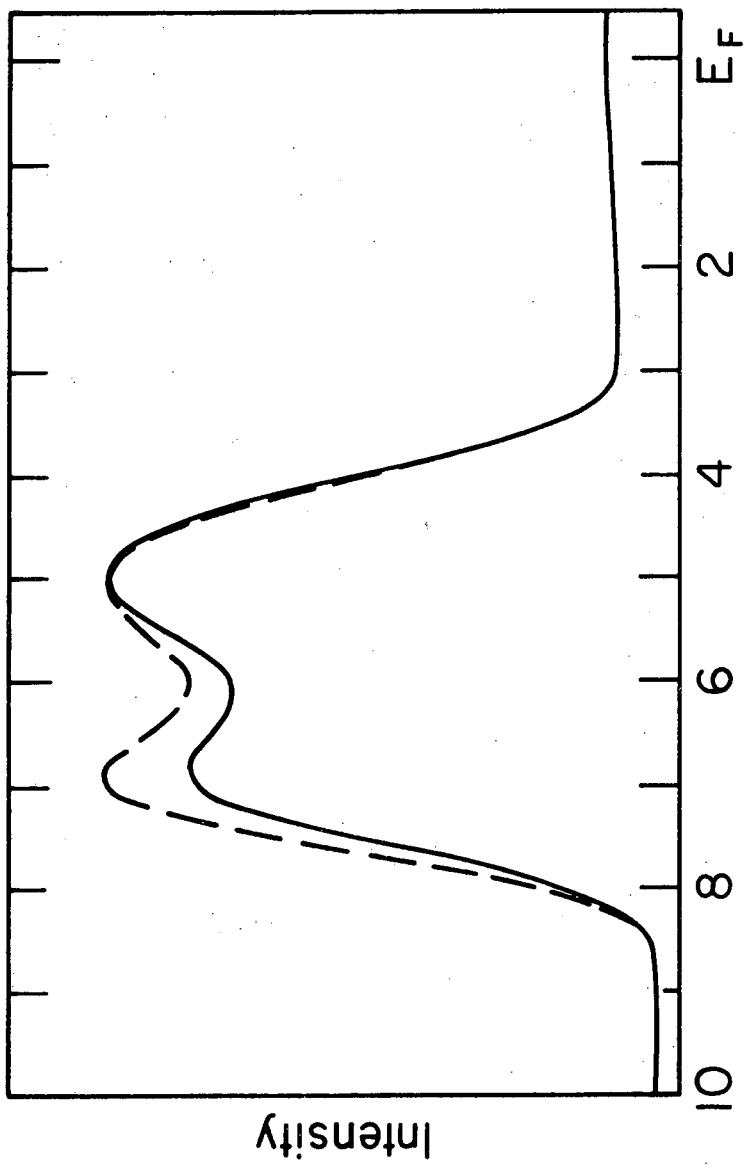

XBL763-2368

Fig. 5

0 0 0 4 5 0 4 0 8 0

LEGAL NOTICE

This report was prepared as an account of work sponsored by the United States Government. Neither the United States nor the United States Energy Research and Development Administration, nor any of their employees, nor any of their contractors, subcontractors, or their employees, makes any warranty, express or implied, or assumes any legal liability or responsibility for the accuracy, completeness or usefulness of any information, apparatus, product or process disclosed, or represents that its use would not infringe privately owned rights.

TECHNICAL INFORMATION DIVISION
LAWRENCE BERKELEY LABORATORY
UNIVERSITY OF CALIFORNIA
BERKELEY, CALIFORNIA 94720